

# Universal Machine Learning Kohn-Sham Hamiltonian for Materials

Yang Zhong<sup>1,2</sup>, Jihui Yang<sup>1,2</sup>, Hongjun Xiang<sup>1,2,\*</sup>, and Xingao Gong<sup>1,2</sup>

<sup>1</sup>*Key Laboratory of Computational Physical Sciences (Ministry of Education), Institute of Computational Physical Sciences, State Key Laboratory of Surface Physics, and Department of Physics, Fudan University, Shanghai, 200433, China*

<sup>2</sup>*Shanghai Qi Zhi Institute, Shanghai, 200030, China*

Email: hxiang@fudan.edu.cn

## Abstract

While density functional theory (DFT) serves as a prevalent computational approach in electronic structure calculations, its computational demands and scalability limitations persist. Recently, leveraging neural networks to parameterize the Kohn-Sham DFT Hamiltonian has emerged as a promising avenue for accelerating electronic structure computations. Despite advancements, challenges such as the necessity for computing extensive DFT training data to explore new systems and the complexity of establishing accurate ML models for multi-elemental materials still exist. Addressing these hurdles, this study introduces a universal electronic Hamiltonian model trained on Hamiltonian matrices obtained from first-principles DFT calculations of nearly all crystal structures on the Materials Project. We demonstrate its generality in predicting electronic structures across the whole periodic table, including complex multi-elemental systems. By offering a reliable efficient framework for computing electronic properties, this universal Hamiltonian model lays the groundwork for advancements in diverse fields related to electronic structures.

## Introduction

The electronic structure<sup>1-5</sup> of materials is crucial in understanding and predicting a wide range of physical properties, including electrical conductivity, optical behavior, mechanical strength, chemical reactivity, and magnetic characteristics. Electronic structure calculations provide insights into the electronic band structures, bonding, and reactivity, enabling the design of new materials and the study of chemical reactions. Among diverse quantum mechanics approaches, density functional theory (DFT)<sup>6-9</sup> has become a widely used computational method in electronic structure calculations since DFT has drastically reduced the computational cost by employing the electron density instead of the many body wave function as the fundamental variable. The price to pay for using the electron density as the fundamental variable is that the Kohn-Sham DFT Hamiltonian is no longer a simple explicit function of the atomic structure, but should be obtained by solving a self-consistent Kohn-Sham equation. However, the computational cost of DFT self-consistent field cycles remains expensive for large systems and/or thousands of structures.

In recent years, the use of neural networks to parameterize the ab initio tight-binding Hamiltonian has emerged as an important and effective method to accelerate electronic structure calculations<sup>10-22</sup>. The ML Hamiltonian models offer a significant advantage in electronic structure calculations by providing a direct mapping from the structure to the self-consistent Hamiltonian matrix. This eliminates the need for time-consuming self-consistent iterations typically required in Kohn-Sham DFT. By bypassing these iterations, the ML Hamiltonian models greatly accelerate the calculation process for large systems and other computationally expensive calculations. Initially, Gaussian process regression (GPR)<sup>10</sup> or multilayer perceptron (MLP)<sup>15</sup> models were employed to fit empirical Hamiltonians for simple systems. Subsequently, invariant graph neural networks<sup>12</sup> were developed to directly fit the ab initio Hamiltonian for molecules and solids. However, invariant graph neural networks approximate the Hamiltonian's equivariance through data augmentation. Recently, building upon equivariant graph neural networks<sup>22</sup>, researchers have further improved the fitting accuracy of the ab initio Hamiltonian and achieved transferable predictions for Hamiltonians containing multiple configurations.

However, there are still several challenges in using machine learning for electronic Hamiltonian prediction. Firstly, exploring a new system often requires conducting a significant number of DFT calculations and retraining a model specifically for that system. Preparing the DFT training data for a specific system is currently not an automatic process and can be time-consuming and computationally expensive, limiting the wide range of use of the approach. Secondly, many materials of practical interest, such as high-entropy alloys<sup>23-25</sup> and ceramics<sup>26, 27</sup>, consist of a large number of elements, making it challenging to establish accurate machine-learning models for their electronic Hamiltonians as a huge amount of DFT training data is needed. Current research efforts have primarily focused on systems containing no more than three elements, and extending this to more complex systems remains a significant hurdle in the field. Overcoming these challenges is crucial to enable the broader application of machine learning in predicting electronic Hamiltonians for diverse and multi-elemental materials. Recently, several groups reported developments of universal machine learning potentials<sup>28-32</sup>, which can handle almost all elements across the whole periodic table. Naturally, one might wonder whether it is possible to develop a universal machine-learning model for electronic Hamiltonians. Such a model would enable efficient and accurate calculations of electronic structures for a wide range of materials and large-scale systems. However, achieving a truly universal model for electronic Hamiltonians poses significant challenges. The inherent complexity and diversity of the electronic behavior in materials are influenced by various factors, including chemical composition, bonding types, crystal structures, and electronic correlations. Designing a single model capable of accurately capturing these diverse phenomena for all materials appears to be a formidable task. Moreover, the availability of high-quality training data for such a universal model seems to be another major hurdle.

In this work, we propose a universal Kohn-Sham Hamiltonian model in the sense that this single model is applicable to all elements of the entire periodic table and all structures of a given chemical composition. This is achieved by training on Hamiltonian

matrices obtained from first-principles calculations of nearly all crystal structures on the Materials Project<sup>33, 34</sup>. The universal nature of our ML model is demonstrated by its successful prediction of the electronic structures for various bulk or low-dimensional materials with different combinations of chemical elements in the periodic table. The universal model successfully captures not only common systems but also those containing uncommon or rare transition metal elements. Furthermore, it proves high accuracy even in complex multi-element systems comprising more than five elements. By providing a reliable framework for understanding electronic properties across the periodic table, this research paves the way for advancements in material design, catalysis, electronics, and other fields that heavily rely on efficient predictions of electronic structures.

## Results

---

### *The framework of the universal electronic Hamiltonian model*

Constructing an ML model for the electronic Hamiltonian is more complicated than constructing machine learning interatomic potentials (MLIPs)<sup>35-41</sup>. MLIPs provide a mapping from the two degrees of freedom, atomic types  $\{Z_i\}$  and atomic positions  $\{\mathbf{r}_i\}$ , to the scalar potential energy  $E$ . In addition to the two degrees of freedom, the mapping from a crystal structure to the electronic Hamiltonian matrix also necessitates handling the supplementary degree of freedom arising from distinct atomic orbital bases  $\{\phi_{i\alpha}\}$  associated with each atom. As the number of elements in the system increases, the relevant degrees of freedom and interactions in the electronic Hamiltonian matrix also increase dramatically, leading to a significant increase in complexity when fitting the electronic Hamiltonian matrix. Therefore, a universal electronic Hamiltonian model across the periodic table requires much more network capacity than the MLIPs to capture all degrees of freedom accurately. For large molecules or crystals, especially in cases where the basis set is large and the system is complex, the dimension of the electronic Hamiltonian matrix can be extremely large. This increases the difficulty of model training, as it requires handling large-scale matrix and storing a significant amount of parameters. In addition, different sub-blocks of a Hamiltonian matrix are subject to different equivariant constraints under a rotation operation, so the Hamiltonian matrix predicted by the model must also adhere to these constraints.

We have trained a universal Hamiltonian model following the process shown in Figure 1. To develop a universal electronic Hamiltonian model for the whole periodic table, we utilized one of the world's largest open databases for DFT-relaxed crystal structures, namely the Materials Project<sup>33, 34</sup>. We used OpenMX<sup>42, 43</sup>, a DFT software package based on norm-conserving pseudopotentials and pseudo-atomic localized basis functions, to calculate the Hamiltonian matrices of approximately 55,000 structures on the Materials Project. Among them, approximately 44,000 structures' Hamiltonian matrices were utilized as a training set, while validation and test sets were created using the Hamiltonian matrices of around 5,500 structures each. Then, we use these datasets to train a universal HamGNN<sup>22</sup> model. HamGNN is a deep learning model based on equivariant graph neural networks, which can automatically learn the

features of each element on the entire periodic table without any prior physical or chemical properties of elements. The architecture of the HamGNN model and the training process are shown in Figure 1(b). We will briefly introduce the principle of HamGNN for predicting the Hamiltonian matrix in the following paragraph, and for more network details see Ref. 22.

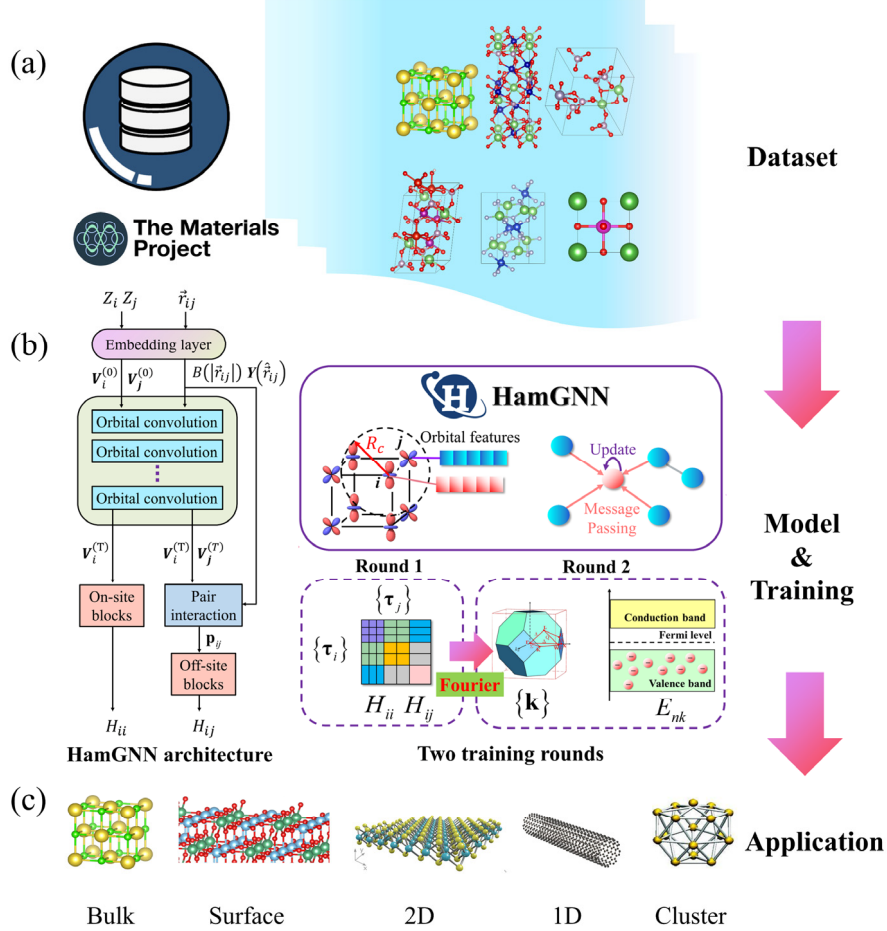


**Figure 1.** The framework of a universal Hamiltonian model based on HamGNN. (a) Training dataset preparation. The training dataset is generated by calculating the real-space Hamiltonian matrices of crystal structures available on the Materials Project using an ab initio tight-binding software based on numerical atomic orbitals. (b) Model architecture and the training procedure. This dataset is utilized for training the HamGNN model, a deep learning approach that employs equivariant graph neural networks to predict the Hamiltonian matrix. The model can automatically learn the intrinsic features of each element on the periodic table solely based on their atomic numbers, without relying on any prior physical or chemical properties. In HamGNN, the orbital features of the central atom are updated by considering interactions between the neighbor atoms within a cutoff radius of  $R_c$ . For atomic pairs beyond this cutoff radius, multi-layer message passing is employed to exchange orbital features. To achieve universality, HamGNN requires two rounds of training. In the first round, the loss function for network training solely considers the error in the real-space Hamiltonian matrix. After this initial round of training, this model can accurately predict the real-space Hamiltonian matrices with high precision. In the second round of training, the real-space Hamiltonian matrices are transformed into the reciprocal Hamiltonian matrices at randomly selected  $\mathbf{k}$  points in the

Brillouin zone, and the errors of the orbital energies near the Fermi level obtained by diagonalizing the reciprocal Hamiltonian matrices are incorporated into the total loss function. (c) Applications of the universal HamGNN model. After two rounds of training, the universality of the HamGNN model has significantly improved, enabling accurate prediction of electronic structures in crystals with arbitrary periodic boundary conditions and any components.

Since the irreducible representations with rotation orders  $l = 0, 1, 2, \dots$  of the  $O(3)$  group possess the same rotational equivariance and parity symmetry as the atomic orbitals  $s, p, d, \dots$ , HamGNN uses a direct sum of equivariant atomic features  $\mathbf{V}_l$  with different rotation orders  $l$  to characterize each atom:  $\mathbf{V} = \mathbf{V}_0 \oplus \mathbf{V}_1 \oplus \dots \oplus \mathbf{V}_{l_{\max}}$ . This feature tensor satisfies the rotational equivariance under the rotation operation  $\hat{R}$ :  $\mathbf{D}(\hat{R})\mathbf{V}$ , where  $\mathbf{D}_l$  ( $l < l_{\max}$ ) is a Wigner  $D$  matrix<sup>44, 45</sup> of order  $l$ . HamGNN updates the equivariant atomic features through an equivariant message-passing function in the orbital convolution layer. After  $T$  orbital convolution layers, the atomic features are transformed into on-site Hamiltonian matrices by an “on-site layer”. HamGNN merges the features of atom pairs  $ij$  into the edge features  $\mathbf{P}_{ij}$  in the “Pair interaction layer”. The edge features  $\mathbf{P}_{ij}$  is later transformed into an off-site Hamiltonian matrix through an “off-site layer”. Each subblock of the Hamiltonian matrix can be decomposed into a set of  $O(3)$  equivariant irreducible spherical tensors (ISTs) according to the following equation<sup>44-47</sup>:

$$l_i \otimes l_j = |l_i - l_j| \oplus |l_i - l_j| + 1 \oplus \dots \oplus |l_i + l_j| \quad (1)$$

The on-site and off-site layers output each sub-block of the Hamiltonian matrix by the following equation

$$H_{l_i m_i, l_j m_j} = \sum_{l=|l_i-l_j|}^{l_i+l_j} \sum_{m=-l}^l C_{m_i, m_j, m}^{l_i, l_j, l} T_m^l \quad (2)$$

where  $T_m^l$  is an equivariant IST with rotation order  $l$  in  $\mathbf{V}_i^{(T)}$  or  $\mathbf{P}_{ij}$ ,  $C_{m_i, m_j, m}^{l_i, l_j, l}$  is the Clebsch-Gordan coefficient.

To achieve a universal model, HamGNN needs to undergo two rounds of training. During the first round of training, only the error of the real-space Hamiltonian matrix is considered as the loss function for the network's training. After the first round of training, this model can accurately predict the real-space Hamiltonian matrix. However, the model still requires further fine-tuning to enhance its accuracy in predicting the electronic eigenvalues of the Bloch states. During each training step in the second round, Fourier transformations are performed on the predicted and target real-space Hamiltonian matrices at randomly selected  $\mathbf{k}$  points in the Brillouin zone. The orbital energies  $\varepsilon_{n\mathbf{k}}$  are obtained by diagonalizing the reciprocal Hamiltonian matrices, and the error of the orbital energies near the Fermi level is incorporated into the loss function as follows:

$$L = \|\tilde{H} - H\| + \frac{\lambda}{N_{orb} \times N_k} \sum_{k=1}^{N_k} \sum_{n=1}^{N_{orb}} \|\tilde{\epsilon}_{nk} - \epsilon_{nk}\| \quad (3)$$

where the variables marked with a tilde refer to the corresponding predictions and  $\lambda$  denotes the loss weight of the orbital energy error.  $N_{orb}$  is the number of orbits selected near the Fermi level,  $N_k$  is the number of the random  $\mathbf{k}$  points generated in each training step.

### Training results on the dataset of Materials Project

Figure 2(a) displays the count of each chemical element in the training set for the Hamiltonian. The metallic elements of Group IA and IIA, as well as the non-metallic elements of Group IVA, VA, VIA, and VIIA, have the highest proportion in the training set. Except for some less common transition metal elements that are not included in the training set, this dataset includes all elements supported by OpenMX's PBE pseudopotential library. After the first round of training, the HamGNN model achieved a mean absolute error (MAE) of only 5.4 meV for the real-space Hamiltonian matrix on the test set. The accuracy of the model for the real-space Hamiltonian matrix is shown in Figure 2(b). In the second round of training, we incorporate the error of orbital energies at five randomly selected  $\mathbf{k}$ -points in the Brillouin zone into the loss function to restart the training, with a  $\lambda$  value set at 0.01. After the second round of model fine-tuning, the generalization ability of the HamGNN model has significantly improved. By addressing potential overfitting issues, this model demonstrates better adaptability to different datasets and real-world scenarios, showcasing enhanced universality and stability. We will evaluate HamGNN's prediction accuracy for various crystals across the entire periodic table in the subsequent discussions.

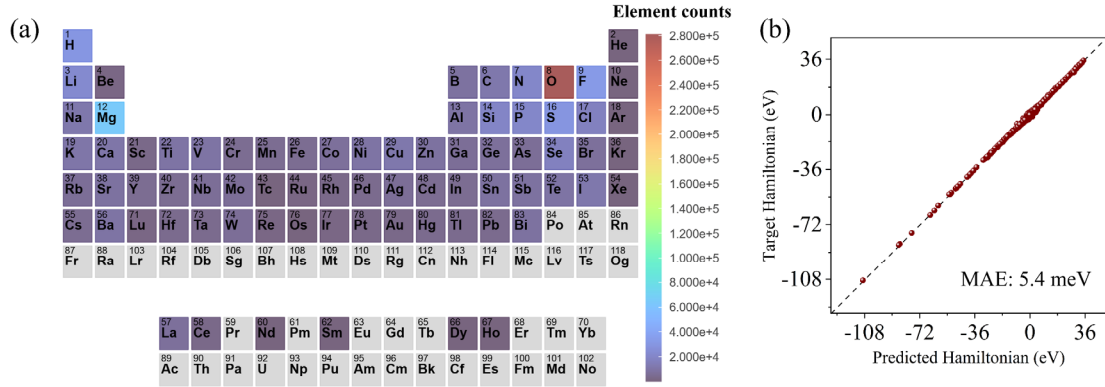


**Figure 2.** (a) The element distribution of the training dataset. (b) The comparison of the Hamiltonian calculated by HamGNN and OpenMX for the test dataset.

To verify the universality and accuracy of our trained universal HamGNN model, we predicted the Hamiltonian matrices for all structures in the test set and obtained band structures through diagonalization of the Hamiltonian matrices. To present the results intuitively, we compared the band structures predicted for four structures in the test set with those calculated using OpenMX, as shown in Figure 3. It is worth noting that the proportions of Zr, Ru, and Tl, three transition metal elements, are relatively low in the training set. However, the universal HamGNN model can still accurately

reproduce the band structures of crystals containing these elements. This indicates that the universal model we have established not only has broad adaptability but also reliably handles crystals containing rare or low-frequency occurring elements.

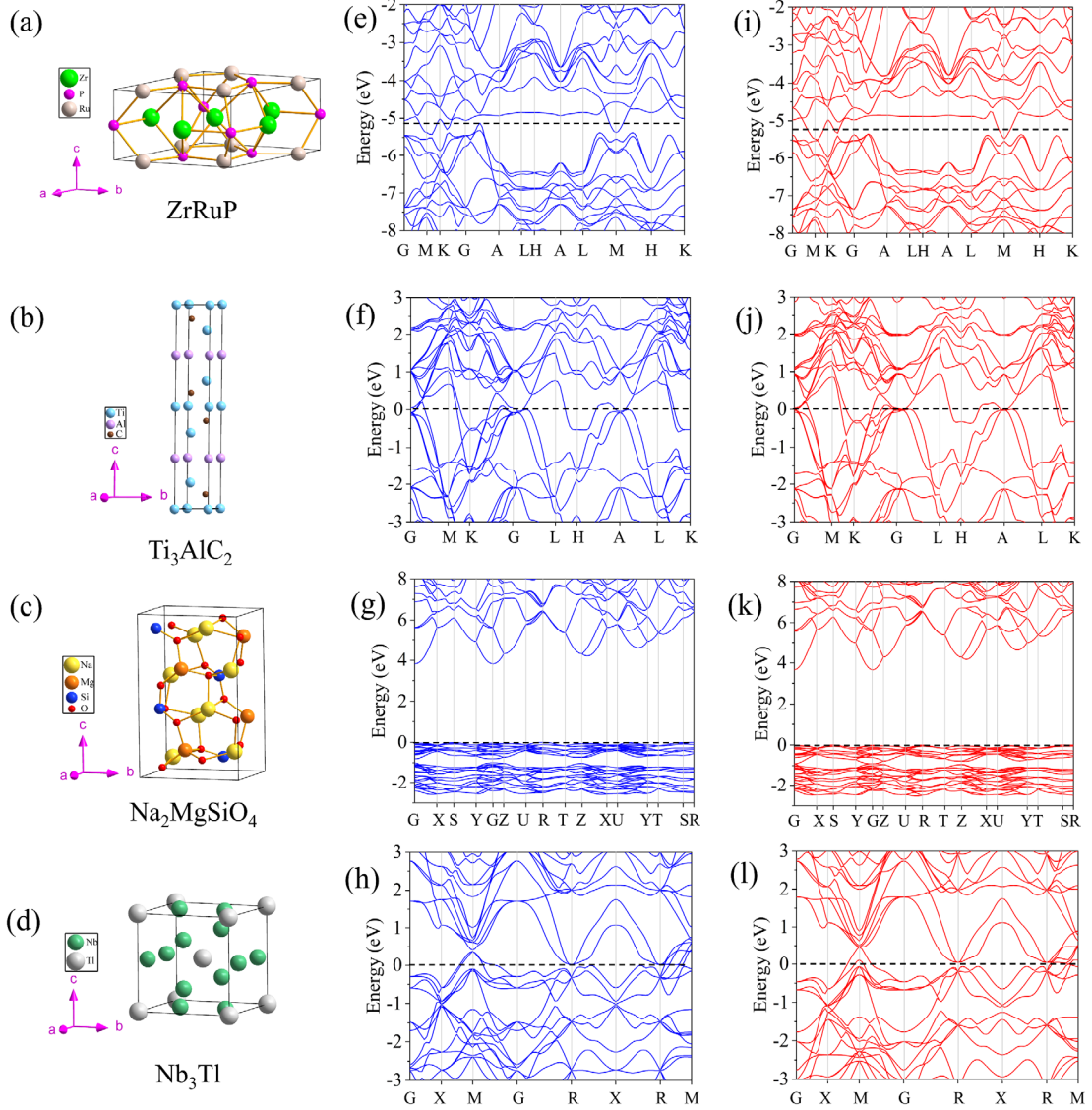


**Figure 3.** Prediction results for four crystals in the test set. Crystal structures of (a) ZrRuP, (b)  $\text{Ti}_3\text{AlC}_2$ , (c)  $\text{Na}_2\text{MgSiO}_4$ , and (d)  $\text{Nb}_3\text{Ti}$ . Predicted band structures of (e) ZrRuP, (f)  $\text{Ti}_3\text{AlC}_2$ , (g)  $\text{Na}_2\text{MgSiO}_4$ , and (h)  $\text{Nb}_3\text{Ti}$ . Band structures calculated by OpenMX for (i) ZrRuP, (j)  $\text{Ti}_3\text{AlC}_2$ , (k)  $\text{Na}_2\text{MgSiO}_4$ , and (l)  $\text{Nb}_3\text{Ti}$ .

### Testing on multi-element materials

We are now applying our universal electronic Hamiltonian model to systems that are not included in the Materials Project in order to test the versatility of our model. Previous ML Hamiltonian models<sup>10, 15, 20</sup> typically handle crystal structures composed of only 1 to 3 elements, and training an accurate model that can deal with complex crystal structures containing more elements is challenging. The training datasets commonly used by these models are built from structures perturbed using molecular dynamics. However, as the number of atomic species in the crystal increases, the degrees of freedom of the Hamiltonian matrix increase sharply. Consequently, the



training samples generated by perturbing a seed structure cannot fully cover the entire configuration space of the crystal. In these cases, the perturbed structures often contain many similar and repetitive patterns, which can cause the Hamiltonian model to be trapped in local minima and fail to accurately fit the Hamiltonian of crystals with multiple elements and complex configurations. However, the universal Hamiltonian model can effectively address such concerns. Through extensive training on a comprehensive and diverse dataset, the universal Hamiltonian model develops a profound understanding of the intricate interactions among atoms in various configurations.

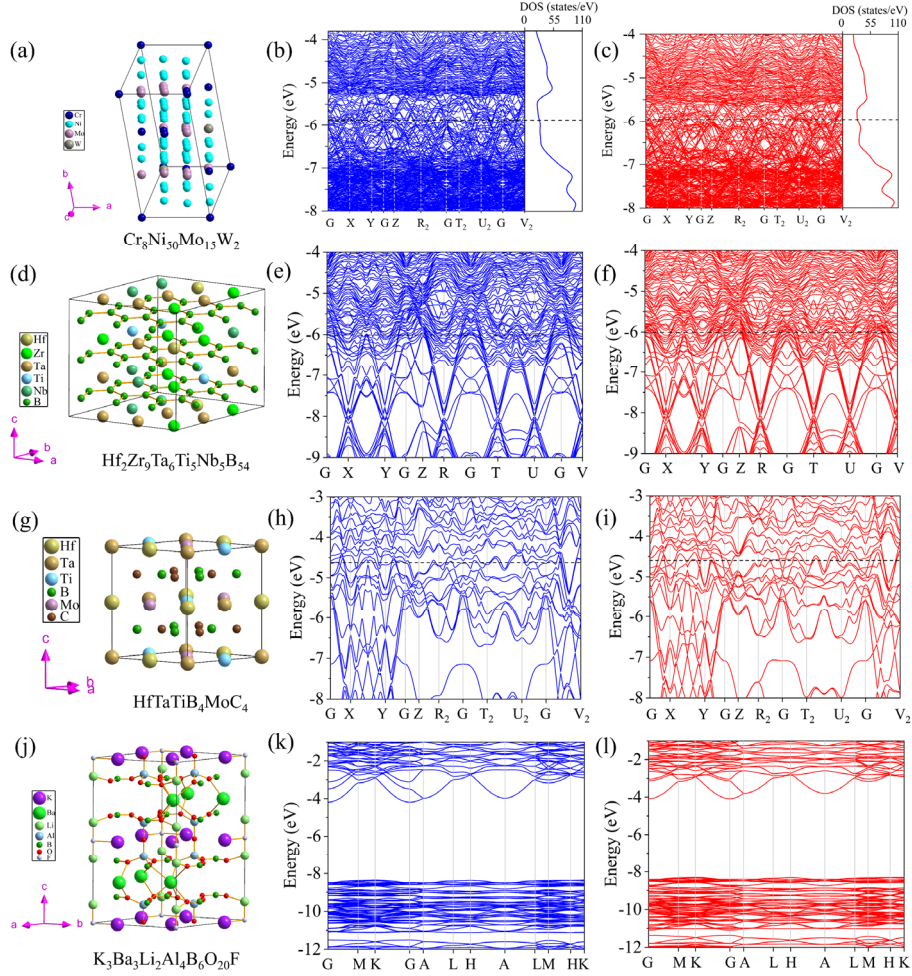


**Figure 4.** The crystal structures of (a)  $\text{Cr}_8\text{Ni}_{50}\text{Mo}_{15}\text{W}_2$ , (d)  $\text{Hf}_2\text{Zr}_9\text{Ta}_6\text{Ti}_5\text{Nb}_5\text{B}_{54}$ , (g)  $\text{HfTaTiB}_4\text{MoC}_4$ , and (j)  $\text{K}_3\text{Ba}_3\text{Li}_2\text{Al}_4\text{B}_6\text{O}_{20}\text{F}$ . The predicted (blue line) and calculated (red line) energy bands of (b,c)  $\text{Cr}_8\text{Ni}_{50}\text{Mo}_{15}\text{W}_2$ , (e,f)  $\text{Hf}_2\text{Zr}_9\text{Ta}_6\text{Ti}_5\text{Nb}_5\text{B}_{54}$ , (h,i)  $\text{HfTaTiB}_4\text{MoC}_4$ , and (k,l)  $\text{K}_3\text{Ba}_3\text{Li}_2\text{Al}_4\text{B}_6\text{O}_{20}\text{F}$ .

The universal HamGNN's generalization performance and accuracy were evaluated by conducting tests on four different crystal structures:  $\text{Cr}_8\text{Ni}_{50}\text{Mo}_{15}\text{W}_2$ ,  $\text{Hf}_2\text{Zr}_9\text{Ta}_6\text{Ti}_5\text{Nb}_5\text{B}_{54}$ ,  $\text{HfTaTiB}_4\text{MoC}_4$ , and  $\text{K}_3\text{Ba}_3\text{Li}_2\text{Al}_4\text{B}_6\text{O}_{20}\text{F}$ . These crystals were specifically chosen to represent a diverse range of compositions and structural complexities<sup>48-50</sup>.  $\text{Cr}_8\text{Ni}_{50}\text{Mo}_{15}\text{W}_2$  is a disordered alloy containing four elements, and



its crystal structure belongs to the  $P1$  space group of the triclinic crystal system. Its unique structure makes it have good corrosion resistance and high-temperature stability, so it can be regarded as a potential material for superalloys, acid-resistant materials, etc. The compound  $\text{Hf}_2\text{Zr}_9\text{Ta}_6\text{Ti}_5\text{Nb}_5\text{B}_{54}$  exhibits a hexagonal  $\omega$ -phase derived structure and belongs to the  $P1$  space group of the triclinic crystal system. It consists of five distinct metal ions, which are inserted into the gaps between the hexagonal monolayers of boron.  $\text{HfTaTiB}_4\text{MoC}_4$  crystallizes in the triclinic  $P1$  space group, with the metal elements inserted into the gaps between the hexagonal monolayers composed of boron and carbon.  $\text{K}_3\text{Ba}_3\text{Li}_2\text{Al}_4\text{B}_6\text{O}_{20}\text{F}$  is a deep ultraviolet transparent nonlinear optical crystal, composed of seven elements and possessing a large bandgap<sup>51</sup>.

To assess the generalization performance of HamGNN, a comparison was made between the predicted energy bands generated by the model and the calculated energy bands by OpenMX for each of these four crystals, as shown in Figure 4. By examining Figure 4, it becomes evident that HamGNN demonstrates remarkable generalizability in predicting the energy bands for the four crystal structures. The predicted energy bands align closely with the calculated ones, indicating that HamGNN is capable of accurately capturing the electronic properties of these materials. This successful evaluation highlights the effectiveness and reliability of HamGNN as a universal model for predicting electronic structures across various crystal systems. Its ability to generalize well across different compositions and structural complexities makes it an invaluable tool in high-throughput electronic structure calculations for the periodic table.

### ***Tests on low-dimensional materials***

The above discussions have demonstrated the accuracy of the universal HamGNN model on bulk materials. Now, we will further explore its generalizability and prediction accuracy in the field of low-dimensional materials. We constructed a two-dimensional heterostructure consisting of  $\text{MoS}_2/\text{WS}_2$  with a twist angle of  $3.5^\circ$ , as shown in Figure 5(a) and Figure 5(b). This structure comprises 1625 atoms and exhibits a higher level of complexity compared to the bulk structures typically included in our training set. The universal HamGNN model effectively captures the interatomic interactions within the bilayer  $\text{MoS}_2/\text{WS}_2$  heterostructure and demonstrates excellent agreement between the energy bands predicted by the universal HamGNN model (Figure 5(c)) and those calculated by OpenMX (Figure 5(d)). The universal HamGNN model was further tested on the C60 cluster. Figure 5(e) demonstrates a good alignment between the predicted energy level of the C60 cluster near the band gap and the results obtained through DFT calculations, while Figure 5(f) illustrates a close match between the predicted wave function and the wave function calculated by DFT. These tests demonstrate the powerful and wide applicability of the universal HamGNN model in various material systems, ranging from bulk crystals to low-dimensional materials. By utilizing this universal model, researchers can now explore a vast array of low-dimensional materials with tailored functionalities and properties.

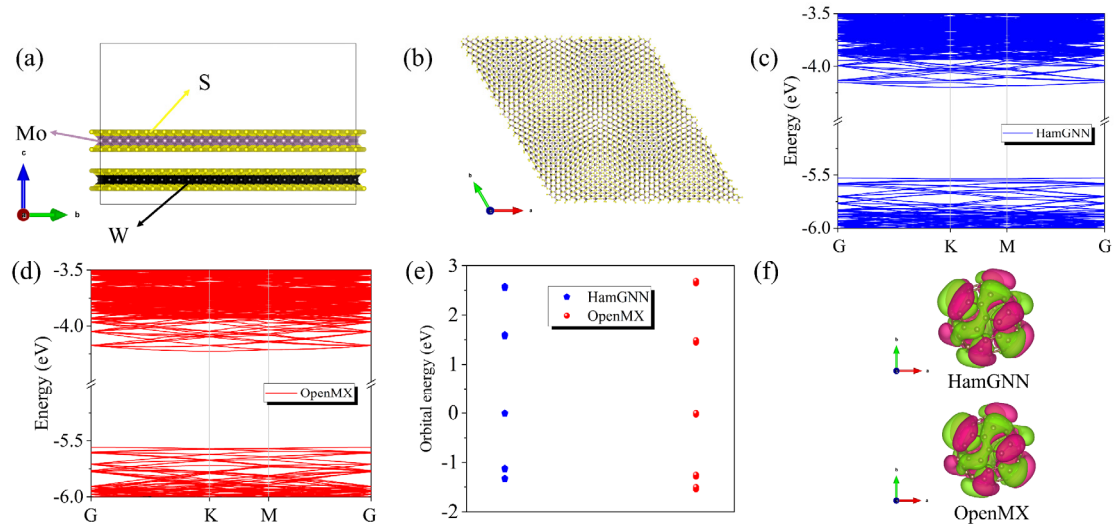


**Figure 5.** Prediction results of the universal HamGNN model for the bilayer  $\text{MoS}_2/\text{WS}_2$  heterostructure with a twist angle of  $3.5^\circ$  and the C60 cluster. (a) Side view of the bilayer  $\text{MoS}_2/\text{WS}_2$  heterostructure. (b) Top view of the bilayer  $\text{MoS}_2/\text{WS}_2$  heterostructure. (c) Predicted band structure of the bilayer  $\text{MoS}_2/\text{WS}_2$  heterostructure. (d) Band structure of the bilayer  $\text{MoS}_2/\text{WS}_2$  heterostructure calculated by OpenMX. (e) The HamGNN-predicted and OpenMX-calculated orbital energies for the C60 cluster. (f) The HamGNN-predicted and OpenMX-calculated wavefunction for the highest occupied molecular orbital (HOMO) of the C60 cluster.

## Discussion

This work not only achieves a universal electronic Hamiltonian model for the entire periodic table but also demonstrates its practicality and reliability through successful predictions of electronic structures in various materials. By training on Hamiltonian matrices obtained from first-principles calculations of nearly all crystal structures on the Materials Project, the model can accurately capture not only common systems but also those containing uncommon or rare transition metal elements. One notable advantage of this universal model is its ability to handle complex multi-element systems comprising more than five elements. This capability opens up new possibilities for studying and understanding the electronic properties of advanced materials that often involve intricate combinations of chemical elements. The reliable framework provided by the universal electronic Hamiltonian model allows for efficient predictions of electronic structures across the periodic table. This breakthrough has significant implications for material design, catalysis, electronics, and other fields that heavily rely on accurate knowledge and understanding of electronic properties. In this work, we consider the Kohn-Sham electronic Hamiltonians for spin-unpolarized systems. Our ML framework for universal electronic Hamiltonians can be straightforwardly extended to systems where spin-orbit coupling or magnetism is important to their electronic structures in the future.

## Methods

### Network details.

The equivariant node features are  $32 \times 0o + 128 \times 0e + 128 \times 1o + 64 \times 1e + 128 \times 2e + 32 \times 2o + 64 \times 3o + 32 \times 3e + 32 \times 4o + 32 \times 4e + 16 \times 5o + 8 \times 5e + 8 \times 6e$ , where ‘ $32 \times 0o$ ’ means that there are 32 channels in this feature part, and the features in each channel are O(3) irreducible representations with  $l = 0$  and odd parity. The node features utilized in this universal HamGNN model surpass those employed in our previous work<sup>22</sup> to enhance the network capacity for describing the entire periodic table. The universal HamGNN model has five orbital convolution layers. The spherical harmonic basis functions used to expand the interatomic directions are  $0e + 1o + 2e + 3o + 4e + 5o + 6e$ . The interatomic distance between atom  $i$  and its neighboring atom  $j$ , which falls within the cutoff radius  $r_c$ , is expanded utilizing the Bessel basis function:

$$B(|\tau_{ij}|) = \sqrt{\frac{2}{r_c}} \frac{\sin(n\pi |\tau_{ij}|/r_c)}{|\tau_{ij}|} \quad (4)$$

The atomic neighbors are determined based on the cutoff radius of each atom's orbital basis. The interatomic distance is expanded using a series of Bessel functions with  $n = 1, 2, \dots, N_b$ , where  $N_b$  represents the number of Bessel basis functions. In this study,  $N_b$  is set to 64.

### DFT details.

All the Hamiltonian matrices in the training set were computed using the PBE functional, with a Monkhorst-pack grid of  $6 \times 6 \times 6$ , and a convergence criterion of  $1.0 \times 10^{-8}$  Hartree.

## Reference

1. Marzari, N., Ferretti, A. & Wolverton, C. Electronic-structure methods for materials design. *Nat. Mater.* **20**, 736-749 (2021).
2. McCardle, K. Predicting electronic structure calculation results. *Nat. Comput. Sci.* **3**, 915-915 (2023).
3. Chen, Z. et al. Evolution of the electronic structure in open-shell donor-acceptor organic semiconductors. *Nat. Commun.* **12**, 5889 (2021).
4. Dzade, N. Y. First-principles insights into the electronic structure, optical and band alignment properties of earth-abundant Cu(2)SrSnS(4) solar absorber. *Sci. Rep.* **11**, 4755 (2021).
5. Reidy, K. et al. Direct imaging and electronic structure modulation of moire superlattices at the 2D/3D interface. *Nat. Commun.* **12**, 1290 (2021).
6. Pederson, R., Kalita, B. & Burke, K. Machine learning and density functional theory. *Nat. Rev. Phys.* **4**, 357-358 (2022).
7. Schleider, G. R., Padilha, A. C. M., Acosta, C. M., Costa, M. & Fazzio, A. From DFT to machine learning: recent approaches to materials science—a review. *J. Phys.: Mater.* **2**, (2019).

8. Makkar, P. & Ghosh, N. N. A review on the use of DFT for the prediction of the properties of nanomaterials. *RSC Adv.* **11**, 27897-27924 (2021).
9. Jones, R. O. Density functional theory: Its origins, rise to prominence, and future. *Rev. Mod. Phys.* **87**, 897-923 (2015).
10. Hegde, G. & Bowen, R. C. Machine-learned approximations to Density Functional Theory Hamiltonians. *Sci. Rep.* **7**, 42669 (2017).
11. Li, H. C., Collins, C., Tanha, M., Gordon, G. J. & Yaron, D. J. A Density Functional Tight Binding Layer for Deep Learning of Chemical Hamiltonians. *J. Chem. Theory. Comput.* **14**, 5764-5776 (2018).
12. Schutt, K. T., Gastegger, M., Tkatchenko, A., Muller, K. R. & Maurer, R. J. Unifying machine learning and quantum chemistry with a deep neural network for molecular wavefunctions. *Nat. Commun.* **10**, 5024 (2019).
13. Gastegger, M., McSloy, A., Luya, M., Schutt, K. T. & Maurer, R. J. A deep neural network for molecular wave functions in quasi-atomic minimal basis representation. *J. Chem. Phys.* **153**, 044123 (2020).
14. Unke, O. T. et al. SE(3)-equivariant prediction of molecular wavefunctions and electronic densities. Preprint at <https://ui.adsabs.harvard.edu/abs/2021arXiv210602347U> (2021).
15. Wang, Z. F. et al. Machine learning method for tight-binding Hamiltonian parameterization from ab-initio band structure. *Npj Comput. Mater.* **7**, 11 (2021).
16. Westermayr, J. & Maurer, R. J. Physically inspired deep learning of molecular excitations and photoemission spectra. *Chem. Sci.* **12**, 10755-10764 (2021).
17. Li, H. et al. Deep-learning density functional theory Hamiltonian for efficient ab initio electronic-structure calculation. *Nat. Comput. Sci.* **2**, 367-377 (2022).
18. Nigam, J., Willatt, M. J. & Ceriotti, M. Equivariant representations for molecular Hamiltonians and N-center atomic-scale properties. *J. Chem. Phys.* **156**, 014115 (2022).
19. Schattauer, C., Todorović, M., Ghosh, K., Rinke, P. & Libisch, F. Machine learning sparse tight-binding parameters for defects. *Npj Comput. Mater.* **8**, 116 (2022).
20. Zhang, L. et al. Equivariant analytical mapping of first principles Hamiltonians to accurate and transferable materials models. *npj Comput. Mater.* **8**, 158 (2022).
21. Gong, X. et al. General framework for E(3)-equivariant neural network representation of density functional theory Hamiltonian. *Nat Commun* **14**, 2848 (2023).
22. Zhong, Y., Yu, H., Su, M., Gong, X. & Xiang, H. Transferable equivariant graph neural networks for the Hamiltonians of molecules and solids. *npj Comput. Mater.* **9**, 182 (2023).
23. Ye, Y. F., Wang, Q., Lu, J., Liu, C. T. & Yang, Y. High-entropy alloy: challenges and prospects. *Mater. Today* **19**, 349-362 (2016).
24. Feng, R. et al. High-throughput design of high-performance lightweight high-entropy alloys. *Nat Commun* **12**, 4329 (2021).
25. George, E. P., Raabe, D. & Ritchie, R. O. High-entropy alloys. *Nat. Rev. Mater.* **4**, 515-534 (2019).
26. Zhang, R.-Z. & Reece, M. J. Review of high entropy ceramics: design, synthesis, structure and properties. *J. Mater. Chem. A* **7**, 22148-22162 (2019).
27. Oses, C., Toher, C. & Curtarolo, S. High-entropy ceramics. *Nat. Rev. Mater.* **5**, 295-309 (2020).
28. Zhao, P., Xiao, C. & Yao, W. Universal superlattice potential for 2D materials from twisted

- interface inside h-BN substrate. *npj 2D Mater. Appl.* **5**, 38 (2021).
29. Chen, C. e. a. Expanding materials science with universal many-body graph neural networks. *Nat. Comput. Sci.* **2**, 703-704 (2022).
  30. Chen, C. & Ong, S. P. A universal graph deep learning interatomic potential for the periodic table. *Nat. Comput. Sci.* **2**, 718-728 (2022).
  31. Takamoto, S. et al. Towards universal neural network potential for material discovery applicable to arbitrary combination of 45 elements. *Nat. Commun.* **13**, 2991 (2022).
  32. Deng, B. et al. CHGNet as a pretrained universal neural network potential for charge-informed atomistic modelling. *Nat. Mach. Intell.* **5**, 1031-1041 (2023).
  33. Jain, A. et al. Commentary: The Materials Project: A materials genome approach to accelerating materials innovation. *APL Mater.* **1**, 011002 (2013).
  34. Jain, A. et al., The Materials Project: Accelerating Materials Design Through Theory-Driven Data and Tools. In *Handbook of Materials Modeling*, 2018; pp 1-34.
  35. Wang, H., Zhang, L. F., Han, J. Q. & E, W. N. DeePMD-kit: A deep learning package for many-body potential energy representation and molecular dynamics. *Comput. Phys. Commun.* **228**, 178-184 (2018).
  36. Behler, J. Atom-centered symmetry functions for constructing high-dimensional neural network potentials. *J. Chem. Phys.* **134**, 074106 (2011).
  37. Chmiela, S. et al. Machine Learning of Accurate Energy-Conserving Molecular Force Fields. *Sci. Adv.*, e1603015 (2017).
  38. Pinheiro, M., Ge, F. C., Ferre, N., Dral, P. O. & Barbatti, M. Choosing the right molecular machine learning potential. *Chem. Sci.* **12**, 14396-14413 (2021).
  39. Xie, T. & Grossman, J. C. Crystal Graph Convolutional Neural Networks for an Accurate and Interpretable Prediction of Material Properties. *Phys. Rev. Lett.* **120**, 145301 (2018).
  40. Chmiela, S. et al. Machine learning of accurate energy-conserving molecular force fields. *Sci. Adv.* **3**, e1603015 (2017).
  41. Glielmo, A., Sollich, P. & De Vita, A. Accurate interatomic force fields via machine learning with covariant kernels. *Phys. Rev. B* **95**, 214302 (2017).
  42. Ozaki, T. & Kino, H. Numerical atomic basis orbitals from H to Kr. *Phys. Rev. B* **69**, 195113 (2004).
  43. Ozaki, T. Variationally optimized atomic orbitals for large-scale electronic structures. *Phys. Rev. B* **67**, 155108 (2003).
  44. Weinert, U. Spherical Tensor Representation. *Arch. Ration. Mech. An.* **74**, 165-196 (1980).
  45. Morrison, M. A. & Parker, G. A. A Guide to Rotations in Quantum-Mechanics. *Aust. J. Phys.* **40**, 465-497 (1987).
  46. Grisafi, A., Wilkins, D. M., Csanyi, G. & Ceriotti, M. Symmetry-Adapted Machine Learning for Tensorial Properties of Atomistic Systems. *Phys. Rev. Lett.* **120**, 036002 (2018).
  47. Thomas, N. et al. Tensor field networks: Rotation- and translation-equivariant neural networks for 3D point clouds. Preprint at <https://arxiv.org/abs/1802.08219v3> (2018).
  48. Zeng, L. et al. Superconductivity and non-trivial band topology in high-entropy carbonitride  $\text{Ti}_{0.2}\text{Nb}_{0.2}\text{Ta}_{0.2}\text{Mo}_{0.2}\text{W}_{0.2}\text{C}_{1-x}\text{N}_x$ . *The Innovation Materials* **1**, 100042 (2023).
  49. Zeng, L. et al. Superconductivity in the High-Entropy Ceramics  $\text{Ti}_{0.2}\text{Zr}_{0.2}\text{Nb}_{0.2}\text{Mo}_{0.2}\text{Ta}_{0.2}\text{C}_x$  with Possible Nontrivial Band Topology. *Adv. Sci.* **11**, e2305054 (2024).

50. Zeng, L. et al. Discovery of the High-Entropy Carbide Ceramic Topological Superconductor Candidate  $\text{Ti}_{0.2}\text{Zr}_{0.2}\text{Nb}_{0.2}\text{Mo}_{0.2}\text{Ta}_{0.2}\text{C}$ . *Adv. Funct. Mater.* **33**, 2301929 (2023).
51. Zhao, S. et al. Designing a Beryllium-Free Deep-Ultraviolet Nonlinear Optical Material without a Structural Instability Problem. *J. Am. Chem. Soc.* **138**, 2961-2964 (2016).